A&A 366, 752–764 (2001)
DOI: 10.1051/0004-6361:20010014

Astronomy & Astrophysics

The LMC eclipsing binary HV 2274 revisited

M. A. T. Groenewegen[1,3] and M. Salaris[2,1]

[1] Max-Planck-Institut für Astrophysik, Karl-Schwarzschild-Straße 1, 85740 Garching, Germany
[2] Astrophysics Research Institute, Liverpool John Moores University, Twelve Quays House, Egerton Wharf, Birkenhead CH41 1LD, UK
[3] *Current address:* European Southern Observatory, EIS-team, Karl-Schwarzschild-Straße 2, 85740 Garching, Germany

Received 2 October 2000 / Accepted 13 November 2000

Abstract. We reanalyse the UV/optical spectrum and optical broad-band data of the eclipsing binary HV 2274 in the LMC, and derive its distance following the method given by Guinan et al. (1998a,1998b) of fitting theoretical spectra to the stars' UV/optical spectrum plus optical photometry. We describe the method in detail, pointing out the various assumptions that have to be made; moreover, we discuss the systematic effects of using different sets of model atmospheres and different sets of optical photometric data. It turns out that different selections of the photometric data, the set of model atmospheres and the constraints on the value of the ratio of selective to total extinction in the V-band, result in a 25% range in distances (although some of these models have a large χ^2). For our best choice of these quantities the derived value for the reddening to HV 2274 is $E(B-V) = 0.103 \pm 0.007$, and the de-reddened distance modulus is $DM = 18.46 \pm 0.06$; the DM to the center of the LMC is found to be 18.42 ± 0.07. This is significantly larger than the DM of 18.30 ± 0.07 derived by Guinan et al. (1998a).

Key words. binaries: eclipsing – stars: distances – stars: individual (HV 2274) – Magellanic Clouds – distance scale

1. Introduction

The distance to the Large Magellanic Cloud (LMC) is a fundamental step in the cosmological distance ladder, since the extragalactic distance scale is usually determined with respect to the LMC distance. In fact, both the HST H_0 Key Project (Kennicutt et al. 1995; Freedman et al. 1999) and the Supernovae Calibration Team (Saha et al. 1999) fix the zero-point of the cosmological distance scale assuming a de-reddened LMC distance modulus (DM) of 18.50; in the case of the HST H_0 Key Project the adopted uncertainty of ± 0.13 on the LMC distance modulus represents the largest contribution to their systematic error budget.

In recent years various methods have yielded LMC distance moduli showing a remarkable spread, ranging from $DM = 18.07$ (Udalski et al. 1998a) to $DM = 18.70$ (Feast & Catchpole 1997) – see for example the review by Gibson (1999) or Feast (2001). This uncertainty alone on the LMC distance causes an indetermination by ∼20% on the value of the Hubble constant.

A method that, at present, seems to support the short distance scale, involves the analysis of the light-curve, radial velocity curve and UV/optical spectrum of the detached eclipsing binary HV 2274 in the LMC. It is considered (see, e.g., Gibson 1999) to be one of the most promising techniques to derive a precise distance to the LMC, and it is based on a very elegant idea. From the analysis of the radial velocity and light-curve one obtains very accurate values for the masses and radii of the two binary components, as well as for the ratio of the effective temperatures. Fitting the UV/optical spectrum with model atmospheres one obtains the reddening, effective temperature and distance. This method, as already stressed, has been put forward as *the* way to obtain a very accurate DM to the LMC, in particular when more systems will be analysed.

Guinan et al. (1998a; hereafter G98a) found $DM = 18.30 \pm 0.07$ (the derived distance modulus to HV 2274 was 18.35 ± 0.07). A geometric correction has been then applied to obtain the distance to the center of the LMC) after applying this technique. More recently Nelson et al. (2000) corrected the G98a value after re-determining the reddening toward HV 2274; they obtained $DM = 18.40 \pm 0.07$, a value only marginally in agreement with the long distance. However, they did not apply the method by G98a, deriving the distance correction only in an indirect way.

Because of the relevance of the method employed by G98a for deriving the LMC distance and in light of the

Send offprint requests to: M. A. T. Groenewegen,
e-mail: mgroenew@eso.org

recent claims by Nelson et al. (2000) for a longer LMC distance, we want in the present paper to re-analyse the fitting procedure of the UV/optical spectrum, and carefully point out the uncertainties of this method. Unfortunately, in their 4-page *Letter*, G98a could not present all the intricate details that *are* involved in the application of this method, but which should be pointed out to the scientific community in order to judge the strengths and weaknesses of this technique (also see Feast 2001). We will also study the sensitivity of the derived distance to both the set of model atmospheres and of optical photometric data employed in the fitting procedure.

In Sect. 2 we present an historical overview of observations and studies related to the HV 2274 distance. In Sects. 3 and 4, we discuss, respectively, the observational data and the method employed for the distance determination. Results are presented in Sect. 5, while a discussion follows in Sect. 6.

2. Historical overview

Watson et al. (1992) presented Johnson BV and Cousins I CCD photometry of HV 2274. The estimated out-of-eclipse magnitudes are $V = 14.16$, $(B-V) = -0.18$ and $(V-I) = -0.08$ with uncertainties of "not as large as 0.1 mag".

Guinan et al. (1998b – hereafter G98b) discussed new observational data of HV 2274. They took IUE UV (1200–3000 Å) spectra and fitted them with Kurucz ATLAS 9 model atmospheres. They also obtained UV spectra (1150–4820 Å) with the HST/FOS spectrograph, and medium resolution spectra with the HST/GHRS to obtain the radial velocity curve. The radial velocity curve and light curve (from Watson et al. 1992) were analysed to provide accurate determinations of (amongst others) the ratio of the effective temperatures and the gravities. Then, using the method outlined below, of fitting the FOS spectrum (plus $(B-V)$, from, in this case, Watson et al.) with model atmospheres taking into account the effect of extinction and using the constraints from the radial velocity and light-curve solution, they derived the microturbulent velocity (assumed equal for the 2 components), $E(B-V)$ and coefficients describing the UV extinction in the HV 2274 line-of-sight, the effective temperature of the primary, the metallicity (assumed equal for the 2 components), and the distance (see Table 2). Considering the fact that HV 2274 was estimated by them to be 1100 pc behind the center of the LMC, they derived a $DM = 18.44 \pm 0.07$.

Then, two papers appeared in the same issue of the Astrophysical Journal, Udalski et al. (1998b; hereafter UPW98) and G98a. The former was a reaction to a *pre-print* version of G98a (`astro-ph/9809132v1`; which quoted $E(B-V) = 0.083 \pm 0.006$, and a DM to the binary of 18.47 ± 0.07) and presented out-of-eclipse OGLE-II $UBVI$ photometry ($V = 14.16 \pm 0.02$, $(B-V) = -0.129 \pm 0.015$, $(V-I) = -0.125 \pm 0.015$, $(U-B) = -0.905 \pm 0.04$) of HV 2274. UPW98 derived the reddening to HV 2274 from $(B-V)$ and $(U-B)$, using the colours of unreddened Galactic B-stars, and assuming the mean LMC reddening line of $E(U-B)/E(B-V) = 0.76$. They derived $E(B-V) = 0.149 \pm 0.015$. They did not repeat the fitting procedure in G98a and G98b, but noted that in the reddest part of the spectrum, near 4800 Å, the reddening is proportional to 3.8 $E(B-V)$ (Udalski et al. hence implicitly assumed a Galactic type reddening curve), and derived a distance modulus that was shorter by $(3.8 \times (0.149 - 0.083) = 0.25$ mag, or $DM = 18.22 \pm 0.13$. They chose not to apply a geometrical correction.

The published version of G98a already considered a preprint version of UPW98, and fitted the FOS spectrum plus B, V data, not from Watson et al. (1992 – as was done in G98b), but already with that from UPW98. They derived $E(B-V) = 0.120 \pm 0.009$ and $DM = 18.35 \pm 0.07$ to HV 2274. This already indicates the sensitivity of the solution to the adopted photometry that is included in the fitting procedure. We remark here that, as mentioned in G98a, it is necessary to include in the fitting procedure photometric data in the wavelength region between 4400 and 5500 Å (hence the use of $(B-V)$ data), otherwise a possible degeneracy between the parameters determining the reddening law and $E(B-V)$ does exist.

Nelson et al. (2000) noted the uncertainty in obtaining "standard" U and B photometry, and criticized UPW98 for using a non-standard U filter and few calibration observations. They obtained UBV photometry of stars in a field around the binary. For HV 2274 they obtained $V = 14.20 \pm 0.006$, $(B-V) = -0.172 \pm 0.013$, $(U-B) = -0.793 \pm 0.027$. The errors came from the rms residuals in the transformation from instrumental magnitudes to the standard system. These colours differ significantly from those of UPW98. Nelson et al. (2000) ascribed this mainly to a difference in the U-filter, and, likely, to a smaller extent, to differences in the B-filter. They then used, similarly to UPW98, $(B-V)$ and $(U-B)$ colours to derive a reddening to HV 2274 of $E(B-V) = 0.088 \pm 0.025$. Without re-doing the analysis of G98a,b they noted that this reddening is almost identical to that in G98b and therefore they suggested that a DM of 18.40 ± 0.07 to the center of the LMC is the appropriate one.

3. The observational data

The calibrated out-of-eclipse FOS spectrum consists of four individual spectra, covering four adjacent wavelength regions spanning the range between approximately 1200 and 4800 Å. The calibrated spectra have been taken from the HST archive and provide with observed wavelength, flux (in erg s^{-1} cm^{-2} Å^{-1}), and the formal error on the flux. The observed wavelengths are transformed to rest wavelengths using the measured radial velocity of the binary system of +312 ($\pm$4) km s^{-1}(see Ribas et al. 2000). It is not clear if this correction was applied by G98a,b or not. We find that we obtain a significantly lower χ^2 including this correction. On the other hand, the resolution of the model atmospheres used is such that it is not necessary

to consider the fact that the 2 binary components have different radial velocities, due to their orbital motion.

Before merging the data of different wavelength regions we have compared the fluxes (with errors) in the overlap regions. We found no reason to scale the different spectra, as possible scaling factors are less than 1%. This possible error is considered later-on in the final error budget.

The final merged spectrum has been rebinned to the wavelength grid of the model atmospheres we will use (see next section), which are at a lower resolution than the FOS spectrum. This step was also performed by G98a,b. For each wavelength point λ_i in the model atmosphere we calculate the weighted mean and error of the flux of the FOS spectrum between $0.5 \times (\lambda_{i-1} + \lambda_i)$ and $0.5 \times (\lambda_i + \lambda_{i+1})$, using linear interpolation to estimate the flux and error at the begin- and end-point. Later on we will argue that these formal errors are likely to be underestimates of the true errors.

As a last step one has to remove data points that are affected by interstellar lines (as was done by G98a,b). In fact, the wavelengths of these points can be read from Fig. 2 in G98a, but also stand out clearly as deviations between the model fit (see below) and the observations. After removing these points the final spectrum used in the model fitting contains 254 data points between 1145 and 4790 Å.

The other observational data needed to apply the method described in G98a,b are broad-band photometry. G98b used $(B-V)$ from Watson et al. (1992), while G98a used $(B-V)$ from UPW98, which has a much smaller error. There is also $(V-I)$ data available from UPW98, which was not used by G98a as additional constraint, but will be used by us together with the UPW98 $(B-V)$. The fact that G98a did not make use of the $(V-I)$ data is surprising as one of the problems in the fitting procedure noted by them is a degeneracy between the parameters determining the reddening law, and $E(B-V)$. An additional constraint at longer wavelengths might therefore be very helpful.

To summarise, the reference observational data we will use consist of 256 observational data points, 254 coming from the binned FOS spectrum after removing points that are contaminated by interstellar lines, $(B-V)$ and $(V-I)$.

Recently, the teams representing the 2MASS $JHK_{\rm s}$ survey (Beichman et al. 1998) and the DENIS $IJK_{\rm s}$ survey (Epchtein et al. 1999; Cioni et al. 2000) released data that contain the Magellanic Cloud area. HV 2274 is not in the DENIS database, but it is in the 2MASS survey. The position quoted is (J2000): RA = 5h02m40.74s, Dec = −68d24m21.46s, with magnitudes $J = 15.152 \pm 0.057$, $H = 15.168 \pm 0.107$ and $K_{\rm s} = 15.520 \pm 0.238$. The 2MASS User Support & Help Desk kindly checked their database to communicate the time of observation to be 1998 Oct. 25, 07h27m30.48s UT. This corresponds to $JD = 245\ 1111.689$. These data can not be used as constraint as it will be argued later that this observation happens to almost coincide with a primary eclipse, and so can not be used to constrain the parameters as determined from the out-of-eclipse FOS spectrum and $UBVI$ photometry.

4. The method

The method employed is essentially identical to that used by G98a,b. Using the constraints that come from the (independent) modelling of the radial velocity and light-curve, model atmospheres are fitted to the (binned) UV FOS spectrum and broad-band data.

In more detail, the total out-of-eclipse flux of the binary at each wavelength bin can be written as (see G98a):

$$f_{\rm model}(\lambda) = \left(\frac{r_{\rm A}}{d}\right)^2 [F^{\rm A}_\lambda + (r_{\rm B}/r_{\rm A})^2 F^{\rm B}_\lambda] \times 10^{-0.4\ E(B-V)\ [k(\lambda-V)+R]} \quad (1)$$

where $r_{\rm A}$ and $r_{\rm B}$ are the radii of, respectively, the primary and secondary component, d is the distance, $F^{\rm A}_\lambda$ and $F^{\rm B}_\lambda$ the emergent fluxes from the two components, R is the ratio of selective to total reddening in V, $E(B-V)$ is the colour excess and $k(\lambda - V)$ is the normalised extinction curve defined as $\frac{E(\lambda-V)}{E(B-V)}$.

The model atmospheres we employed are described below; in general they can be characterised by four parameters: effective temperature, gravity, metallicity and micro-turbulent velocity. The micro-turbulent velocity is fixed at 2 km s^{-1}, following the result of G98a (see below) and is assumed to be the same for both components. The gravity of the two components, the ratio of the stellar radii and the ratio of the effective temperatures follow from the radial velocity and light-curve analysis (see G98a, summarized in Table 1). Furthermore, it is assumed that both components have the same metallicity. This leaves four parameters: the effective temperature of the primary, the metallicity, $E(B-V)$ and the scaling factor $\left(\frac{r_{\rm A}}{d}\right)^2$ from which the distance is derived (d [kpc] $= 70.26/\sqrt{\left(\left(\frac{r_{\rm A}}{d}\right)^2\ 10^{23}\right)}$ for $r_{\rm A} = 9.86\ R_\odot$, see Table 1). The inclusion of the extinction curve in Eq. (1) is an essential ingredient in the procedure, and is discussed in detail below. It involves in our case five additional free parameters.

The procedure is as follows. By considering the constraints listed in Table 1 the nine free parameters are varied so that the following function is minimised:

$$\chi^2 = \left(\frac{(B-V)_{\rm model} - (B-V)_{\rm obs}}{\sigma_{\rm B-V}}\right)^2 + \left(\frac{(V-I)_{\rm model} - (V-I)_{\rm obs}}{\sigma_{\rm V-I}}\right)^2 + \sum\left(\frac{\log f_{\rm model}(\lambda) - \log f_{\rm obs}(\lambda)}{\sigma_{\rm obs}(\lambda)}\right)^2 . \quad (2)$$

We use a Levenberg-Marquardt non-linear least-squares method (Press et al. 1992). The method makes use of the derivatives of χ^2 with respect to the free parameters,

Table 1. Constraints from the binary astrometric analysis

Quantity	Symbol	Value
Effective temperature ratio	$T_{\rm B}/T_{\rm A}$	1.005 ± 0.005
Gravity primary	$\log g_{\rm A}$	3.536 ± 0.027
Gravity secondary	$\log g_{\rm B}$	3.585 ± 0.029
Radius primary	$r_{\rm A}$	$9.86 \pm 0.24\ R_\odot$
Radii ratio	$(r_{\rm B}/r_{\rm A})^2$	0.842 ± 0.019

which are calculated numerically[1]. The errors in the parameters are calculated from the square-root of the diagonal elements of the covariance matrix (see Press et al. 1992).

Before going on discussing the model atmospheres and extinction law adopted in the fitting procedure, we want to comment briefly about the parameters listed in Table 1. They are derived either directly from the light curve analysis (e.g., $T_{\rm B}/T_{\rm A}$) or by combining the results from the light curve analysis with the results from the radial velocity curve solution. In particular, the value of $r_{\rm A}$ is obtained from $r_{\rm A} = r_{\rm f} a$, where a is the orbital semimajor axis derived from the radial velocity curve, and $r_{\rm f}$ the fractional radius derived from the light-curve solution. When performing the light-curve analysis, apart from the need to assume some value for the albedos and gravity-darkening exponents, it is necessary to employ even at this stage theoretical model atmospheres (see, e.g. the discussion in Milone et al. 1992), from which, for example, limb-darkening coefficients are derived; in the case of HV 2274, G98ab used (according to Ribas et al. 2000) a version of the Wilson-Devinney (1971) program that includes the Kurucz ATLAS 9 (see next subsection) model atmosphere routine developed by Milone et al. (1992, 1994). The errors quoted in Table 1 are formal errors obtained from the given set of assumptions made by the authors and from the observational errors. It is dificult to assess the uncertainty on the parameters estimated from the light curve analysis due to uncertainties on model atmospheres. Milone et al. (1992) discussed in detail the case of the eclipsing binary AI Phoenicis; even if the two components of this system are much colder objects than HV 2274, it can be instructive to notice that by changing the underlying model atmospheres (black body, Carbon-Gingerich 1969 models, Kurucz 1979 models, Kurucz 1979 models corrected for the missing ultraviolet opacity) and band passes employed in the light curve analysis, the value of the fractional radii of both components are basically unchanged, while the ratio $T_{\rm B}/T_{\rm A}$ varies at most by $\sim$1.6%.

[1] The derivatives are calculated from

$$f' = \frac{f(x+h) - f(x-h)}{2\,h},$$

where $h = \epsilon\ \ x$. Following the considerations in Press et al. (1992) and numerical experiments, we choose $\epsilon = 0.003$ for the variable effective temperature, $\epsilon = 0.03$ for the variables metallicity and c_4, and $\epsilon = 0.01$ for all others.

4.1. Model atmospheres

We will consider three sets of model atmospheres: (1) the ATLAS 9 models by R. L. Kurucz taken from his homepage (Kurucz 2000); (2) model atmospheres calculated by K. Butler (2000, private communication; Butler et al., in preparation); (3) model atmospheres calculated by I. Hubeny (2000, private communication) using the TLUSTY code (Hubeny 1988; Hubeny & Lanz 1992; Hubeny et al. 1994; Hubeny & Lanz 1995).

These codes are not identical. The ATLAS9 code assumes LTE and uses an iron abundance of A(Fe) = 7.67 (on a scale where $\log H = 12$). There is an offset by 0.16 dex between this value and the recommended value of 7.51 ($\pm$ 0.01) by Grevesse & Noels (1993). The TLUSTY code is a fully line-blanketed NLTE model, with improved continuum opacities with respect to Kurucz (Hubeny, private communication), and uses A(Fe) = 7.50. Unfortunately, the wavelength coverage is only up to 8200 Å and therefore does not cover the entire wavelength range of the I-band. In the code used by Butler, hydrogen and helium are in NLTE, while CNO, Si, Mg and the iron group metals are in LTE. The iron abundance used is A(Fe) = 7.46. There are also differences in the abundances of the other metals, but these are generally smaller.

We considered model atmospheres for the following combination of parameters: $T_{\rm eff}$ = 22 000 and 24 000 K, $\log g$ = 3.5 and 4.0, and metallicity [m/H] = -1.0, -0.5, -0.3 and -0.0. We had access also to ATLAS 9 models with different values of the micro-turbulent velocity, and we left it as a free parameter in some tests we performed, aimed at deriving the sensitivity of $E(B-V)$, distance and $T_{\rm eff}$ on the value of the adopted micro-turbulent velocity. No significant differences were found with respect to the case of fixing this parameter at 2 km s^{-1}, and from now on we will always refer to models computed with this value of the micro-turbulent velocity. G98a left this as a free parameter in their fit and derived 1.9 ± 0.7 km s^{-1}.

In the fitting procedure it is necessary to interpolate among 12 models (2 temperatures $\times$ 2 gravities $\times$ 3 metallicities, picked among the 4 metallicities available). The interpolation is done in log flux, linearly in $T_{\rm eff}$ and $\log g$, and quadratically in metallicity. After the interpolated model is created, a correction is made to enforce flux conservation, which typically amounts to less than 0.5%. The Butler and TLUSTY models are calculated at a higher resolution, and are rebinned to the exact wavelength grid of the Kurucz models.

Although no details are explicitly given in G98a, they refer to Fitzpatrick & Massa (1999) were it is explained that they used the ATLAS 9 code to calculate an extended grid of model atmospheres, for different micro-turbulent velocities. They interpolate quadratically in metallicity and micro-turbulent velocity, and linearly in $\log g$ and $\log T_{\rm eff}$. Fitzpatrick & Massa (1999) state that they use the three metallicities closest to the desired one, which should have been [m/H] = -1.0, -0.5 and 0.0 in their case.

4.2. Theoretical colours

From the theoretically predicted observed flux distribution we also have to calculate broad-band colours and magnitudes to minimize the expression given in Eq. (2). In general a magnitude in a generic bandpass can be written as:

$$m = ZP - 2.5 \times \log\left(\frac{\int f_\lambda R_\lambda \mathrm{d}\lambda}{\int R_\lambda \mathrm{d}\lambda}\right), \quad (3)$$

where ZP is the zero point, R_λ the response function, and f_λ the received flux at earth (see for example Bessell et al. 1998). We adopt the response curves of Bessell (1990) for the standard Johnson-Cousins $UBVI$-system. The zero point calibration is done on a model atmosphere of Vega (taken from the Kurucz homepage; a file dated 17-april-1998, with parameters $T_{\rm eff} = 9550$, $\log g = 3.95$, [m/H] $= -0.5$ and $v_{\rm turb} = 2$ km s^{-1}), scaled to a monochromatic flux at 5556 Å of 3.54 10^{-9} erg/s/cm^2/Å for a 0-magnitude star (Gray 1992). On this scale the V magnitude of Vega is +0.03. The zero points in V, $(U-B)$, $(B-V)$ and $(V-I)$ derived in this way are equal to, respectively, −21.082, −0.457, 0.608 and 1.272 mag. In V this is 0.01 brighter than adopted by Fitzpatrick & Massa (1999) and 0.018 fainter than derived by Bessell et al. (1998), the difference with respect to the former paper being probably due to the fact that we used a more recent Kurucz model atmosphere for Vega. In $(U-B)$, $(B-V)$ and $(V-I)$ the differences in the zero points in the sense "this paper minus Bessell et al. (1998)" are −0.003, +0.002 and +0.004 mag, respectively. To within the listed decimal figures we reproduce the effective wavelengths of the $UBVI$ filters as given by Bessell et al. (1998) for a A0V star.

In case of the 2MASS filter system, we obtained the response curves of the total $JHK_{\rm s}$ system (that is, filter transmission, camera response, dichroic reflectivity, typical atmospheric transmission) from the 2MASS Explanatory Supplement (Cutri et al. 2000 – files labeled "Total Response"). Using the same model for Vega as before, effective wavelengths of, respectively, 1.228, 1.639, 2.152 μm, and ZP's of, respectively, −23.750, −24.857 and −25.916 mag in $JHK_{\rm s}$ are derived.

4.3. The extinction curve

The normalized UV extinction curve $k(\lambda - V)$ is described by the following functional form (see for example, Fitzpatrick & Massa 1990):

$$k(\lambda - V) = c_1 + c_2\, x + c_3/(\gamma^2 + (x - x_0^2/x)^2) + c_4 F(x) \quad (4)$$

with $x = 1/\lambda$ in units of μm^{-1}, and with $F(x) = 0$ for $x < 5.9$ μm^{-1} and

$$F(x) = 0.5392\,(x - 5.9)^2 + 0.05644\,(x - 5.9)^3 \quad (5)$$

for $x \geq 5.9$ μm^{-1}. The choice of this particular form is based upon both physical considerations (e.g. to fit the 2175 Å feature with a Lorentz-like profile) and empirical evidence (see Fitzpatrick & Massa 1990, and references therein for a discussion).

From Eqs. (1) and (4) it is clear that possible degeneracies exist in determining some of these parameters. First of all, R and c_1 are dependent. In fact, G98a,b, fix the selective reddening at a value of 3.1. Secondly, for a fixed R value, there is a degeneracy between c_1 and $\left(\frac{r_{\rm A}}{d}\right)^2$. With all other parameters fixed, any change in c_1 can be countered by an appropriate choice of $\left(\frac{r_{\rm A}}{d}\right)^2$ to give the same model flux. It is therefore surprising to read in G98b that they left free both $\left(\frac{r_{\rm A}}{d}\right)^2$ and c_1, c_2, c_3, c_4. Although it is not explicitly stated in G98a which of the parameters describing the extinction were left free, G98a refer to Fitzpatrick & Massa (1999), where it is noted that "the linear terms are combined", probably referring to c_1 and c_2.

In fact, as was already noted by Fitzpatrick & Massa (1990), there is a strong correlation between c_1 and c_2. From Fitzpatrick (1999, his Eq. (A2)):

$$c_1 = 2.030 - 3.007 \times c_2 \quad (6)$$

with an estimated 1σ dispersion of about 0.15. This was derived for Galactic stars, but Misselt et al. (1999) show that stars in the LMC fall on this relation as well.

There is another correlation that is used by us in order to further constrain the UV extinction curve. From Fitzpatrick (1999, his Eq. (A1)):

$$c_2 = -0.824 + 4.717/R \quad (7)$$

with an estimated 1σ dispersion of 0.12.

G98a,b choose to fix the selective reddening at its mean Galactic value of 3.1. However, even within our Galaxy there is a large spread from 2.2 to 5.8 (quoted in Fitzpatrick 1999). This could also be true for different lines-of-sight towards the LMC, and, in fact, Misselt et al. (1999) derive values for R towards LMC stars that range between 2.16 ± 0.30 and 3.31 ± 0.20.

In our fitting procedure we keep R as a free parameter, fix c_2 at its value determined by Eq. (7) and fix c_1 at its value determined by Eq. (6). Other parameters left free are x_0, γ, c_3 and c_4. The final error budget will take into account the scatter in Eqs. (6, 7). We will also check the influence of fixing $R = 3.1$, and leaving c_2 as a free parameter, as was probably done by G98a.

In the optical and near-infrared (NIR) wavelength range ($1.1 \leq x \leq 3.3$ μm^{-1}) the Galactic extinction curve by O'Donnell (1994) is adopted, which is an improvement over the Cardelli et al. (1989) one; it can be written as:

$$k(\lambda - V) = c_5 + \frac{a(x) - 1 + b(x)/R}{0.0014 + 1.0231/R} \quad (8)$$

with $a(x)$ and $b(x)$ given in O'Donnell (1994). The constant c_5 is introduced by us in order to join the UV and optical extinction curve, but may also be thought of as to allow for a small difference between the Galactic and LMC optical and NIR extinction curve. This joining is done at 3.3 μm^{-1}, which is the blue edge of the wavelength region

Table 2. Previous results

Author	$T_{\rm A}$	[Fe/H]	$E(B-V)$	$\left(\frac{r_{\rm A}}{d}\right)^2$	Extinction parameters
G98b	22690 ± 300	-0.42 ± 0.07	0.086 ± 0.015	$(1.99 \pm 0.13)\ 10^{-23(a)}$	c_1, c_2, c_3, c_4 fitted; R fixed
G98a	23000 ± 180	-0.45 ± 0.06	0.120 ± 0.009	$(2.249 \pm 0.063)\ 10^{-23}$	unclear; R fixed

Note: (a). $\left(\frac{r_{\rm A}}{d}\right)^2$ derived from the quoted distance of 49.8 ± 1.5 kpc. The error from the fitting procedure alone is smaller than this.

Table 3. Fit results: main parameters

Model	$\chi^2_{\rm r}$	$T_{\rm A}$ (K)	[m/H]	$E(B-V)$	$\left(\frac{r_{\rm A}}{d}\right)^2$ (10^{-23})	R	Comments
1	2.18	22982 ± 135	-0.36 ± 0.04	0.109 ± 0.006	2.12 ± 0.06	3.17 ± 0.10	Kurucz, standard errors (s.e.)
2	4.68	22865 ± 133	-0.11 ± 0.04	0.104 ± 0.006	2.16 ± 0.07	3.16 ± 0.11	Butler, s.e.
3	2.71	22486 ± 132	-0.12 ± 0.04	0.097 ± 0.006	2.23 ± 0.07	3.39 ± 0.13	Butler, s.e., without 3830 Å point
4	2.16	22987 ± 135	-0.35 ± 0.04	0.110 ± 0.006	2.12 ± 0.06	3.19 ± 0.12	Kurucz, s.e., without 3830 Å point
5	0.98	22932 ± 195	-0.38 ± 0.07	0.103 ± 0.007	2.05 ± 0.07	3.06 ± 0.14	Kurucz, Reference Model (R.M.)
6	1.22	22467 ± 185	-0.13 ± 0.06	0.094 ± 0.007	2.18 ± 0.09	3.31 ± 0.16	Butler, final errors
7	0.98	22930 ± 195	-0.38 ± 0.07	0.103 ± 0.007	2.08 ± 0.07	3.06 ± 0.14	R.M. with c_1 larger by 0.15
8	0.96	22962 ± 197	-0.44 ± 0.07	0.106 ± 0.007	2.13 ± 0.08	3.24 ± 0.14	R.M. with c_2 larger by 0.12
9	0.98	22877 ± 194	-0.38 ± 0.08	0.102 ± 0.007	2.05 ± 0.07	3.06 ± 0.14	R.M. with $T_{\rm B}/T_{\rm A} = 1.010$
10	0.98	22978 ± 196	-0.38 ± 0.07	0.103 ± 0.007	2.04 ± 0.07	3.03 ± 0.14	R.M. with $\log g_{\rm A} = 3.563$
11	0.98	22949 ± 195	-0.38 ± 0.07	0.103 ± 0.007	2.04 ± 0.07	3.05 ± 0.14	R.M. with $\log g_{\rm B} = 3.605$
12	0.98	22931 ± 195	-0.38 ± 0.07	0.103 ± 0.007	2.03 ± 0.07	3.06 ± 0.14	R.M. with $(r_{\rm B}/r_{\rm A})^2 = 0.861$
13	0.93	22926 ± 200	-0.38 ± 0.07	0.102 ± 0.007	1.98 ± 0.07	3.05 ± 0.15	R.M., flux level FOS spectrum 3% lower
14	1.04	22775 ± 192	-0.29 ± 0.06	0.100 ± 0.007	2.06 ± 0.08	3.26 ± 0.15	R.M., flux level FOS spectrum 1% lower beyond 3240 Å
15	0.98	22954 ± 195	-0.38 ± 0.07	0.105 ± 0.007	2.07 ± 0.07	3.09 ± 0.14	R.M. with $(B-V) = -0.119$
16	0.98	22958 ± 194	-0.37 ± 0.06	0.106 ± 0.007	2.09 ± 0.07	3.12 ± 0.14	R.M. with $(V-I) = -0.115$
17	0.98	23052 ± 202	-0.33 ± 0.06	0.119 ± 0.010	2.24 ± 0.11	3.34 ± 0.16	no $(V-I)$ fitted, R.M.
18	1.31	22972 ± 188	-0.46 ± 0.09	0.076 ± 0.008	1.82 ± 0.04	2.06 ± 0.13	As 17, with TLUSTY
19	1.21	22622 ± 202	-0.09 ± 0.06	0.113 ± 0.011	2.47 ± 0.15	3.70 ± 0.17	As 17, with Butler
20	1.02	22818 ± 201	-0.41 ± 0.07	0.093 ± 0.009	1.96 ± 0.08	2.90 ± 0.20	As 17, $(B-V) = -0.172 \pm 0.013$ as constraint
21	0.95	23107 ± 214	-0.55 ± 0.09	0.102 ± 0.007	2.06 ± 0.03	3.1	As 17, R fixed at 3.1
22	0.96	23178 ± 209	-0.55 ± 0.09	0.106 ± 0.007	2.07 ± 0.03	3.1	As 21, $V = 14.16 \pm 0.02$ as additional constraint

where the extinction curve by O'Donnell (1994) is valid. For given parameters $R, c_3, (c_1, c_2)$, the value of c_5 is determined (the value of c_5 does not depend on c_4). The joining procedure allows only for continuity of the function $k(\lambda - V)$ and not of its derivative. However, as we will see below (Sect. 6.3) there is no change in slope at the joining point. The value of c_5 is generally in the range -0.1 to 0.1 (and in particular -0.006 for the reference model 5) and this is a small correction with respect to the second term in Eq. (8) which typically is 2.4 for $x = 3.3$.

5. Results

In the *reference case* the 254 points of the FOS spectrum plus $(B-V)$ and $(V-I)$ from UPW98 are used as the observational data-set. Free parameters are the effective temperature of the primary, the metallicity, $E(B-V)$, the scaling factor $\left(\frac{r_{\rm A}}{d}\right)^2$, R, x_0, γ, c_3 and c_4. c_1 and c_2 are derived from Eqs. (6, 7); c_5 from the continuity of the extinction and follows from the other parameters. From the model spectrum the values of V, $(U-B)$, $(B-V)$, $(V-I)$ and $JHK_{\rm s}$ for the system are predicted.

Table 2 summarizes the results from G98a,b regarding the most important fit parameters. The main difference is in the derived distance, which resulted from using different (and more accurate) B, V photometry. Our results are listed in Tables 3, 4 and 5 where, respectively, the main fit parameters, the parameters describing the UV extinction curve, and predicted broad-band colours are listed.

Table 4. Fit results: parameters of the UV extinction law

Model	x_0	γ	c_2	c_3	c_4
1	4.68 ± 0.03	1.32 ± 0.11	–	2.09 ± 0.40	0.64 ± 0.07
2	4.69 ± 0.03	1.85 ± 0.15	–	5.14 ± 1.13	0.75 ± 0.08
3	4.71 ± 0.04	2.08 ± 0.18	–	7.63 ± 1.75	0.97 ± 0.10
4	4.68 ± 0.02	1.32 ± 0.11	–	2.10 ± 0.40	0.65 ± 0.07
5	4.67 ± 0.04	1.27 ± 0.16	–	2.03 ± 0.58	0.66 ± 0.10
6	4.70 ± 0.06	2.01 ± 0.26	–	7.12 ± 2.42	0.97 ± 0.14
7	4.67 ± 0.04	1.27 ± 0.16	–	2.03 ± 0.59	0.66 ± 0.10
8	4.67 ± 0.04	1.28 ± 0.17	–	1.93 ± 0.57	0.58 ± 0.10
9	4.67 ± 0.04	1.28 ± 0.16	–	2.05 ± 0.59	0.66 ± 0.10
10	4.67 ± 0.04	1.27 ± 0.15	–	2.00 ± 0.58	0.66 ± 0.10
11	4.67 ± 0.04	1.27 ± 0.15	–	2.03 ± 0.58	0.66 ± 0.10
12	4.67 ± 0.04	1.27 ± 0.15	–	2.02 ± 0.58	0.66 ± 0.10
13	4.67 ± 0.04	1.27 ± 0.16	–	2.03 ± 0.60	0.66 ± 0.11
14	4.69 ± 0.03	1.28 ± 0.15	–	2.18 ± 0.61	0.79 ± 0.11
15	4.67 ± 0.04	1.29 ± 0.15	–	2.04 ± 0.59	0.65 ± 0.10
16	4.67 ± 0.04	1.30 ± 0.14	–	2.06 ± 0.59	0.65 ± 0.10
17	4.68 ± 0.04	1.39 ± 0.17	–	2.21 ± 0.62	0.63 ± 0.09
18	4.57 ± 0.05	1.02 ± 0.18	–	1.30 ± 0.46	0.35 ± 0.12
19	4.74 ± 0.07	2.39 ± 0.32	–	9.70 ± 3.48	0.92 ± 0.13
20	4.67 ± 0.04	1.24 ± 0.16	–	2.07 ± 0.61	0.70 ± 0.13
21	4.66 ± 0.04	1.19 ± 0.15	0.88 ± 0.08	1.62 ± 0.50	0.47 ± 0.11
22	4.66 ± 0.04	1.19 ± 0.15	0.86 ± 0.08	1.55 ± 0.47	0.46 ± 0.11

Table 5. Fit results: colours

Model	V	$(U-B)$	$(B-V)$	$(V-I)$	J	H	K_s
1	14.175	−0.869	−0.124	−0.095	14.476	14.528	14.585
2	14.187	−0.868	−0.137	−0.100	14.509	14.542	14.612
3	14.194	−0.866	−0.142	−0.102	14.516	14.547	14.617
4	14.174	−0.869	−0.123	−0.094	14.475	14.526	14.583
5	14.181	−0.870	−0.130	−0.105	14.503	14.559	14.618
6	14.198	−0.867	−0.145	−0.108	14.532	14.565	14.636
7	14.181	−0.870	−0.130	−0.104	14.503	14.558	14.617
8	14.178	−0.868	−0.128	−0.097	14.482	14.534	14.590
9	14.181	−0.870	−0.130	−0.105	14.503	14.559	14.618
10	14.181	−0.869	−0.131	−0.106	14.506	14.562	14.622
11	14.181	−0.870	−0.130	−0.105	14.504	14.560	14.619
12	14.181	−0.870	−0.130	−0.105	14.504	14.559	14.618
13	14.215	−0.870	−0.131	−0.105	14.538	14.593	14.653
14	14.194	−0.872	−0.132	−0.103	14.510	14.563	14.621
15	14.179	−0.869	−0.128	−0.101	14.495	14.549	14.608
16	14.178	−0.869	−0.127	−0.099	14.489	14.542	14.600
17	14.164	−0.866	−0.115	−0.078	14.434	14.479	14.533
18	14.221	−0.878	−0.161	–	–	–	–
19	14.177	−0.862	−0.128	−0.075	14.445	14.465	14.528
20	14.191	−0.871	−0.139	−0.119	14.540	14.600	14.662
21	14.183	−0.870	−0.132	−0.104	14.503	14.558	14.616
22	14.179	−0.869	−0.129	−0.100	14.492	14.546	14.604

5.1. Models 1–4

The first 4 models provide preliminary results. We have employed the observational data of the reference case with the formal errors derived from the FOS spectrum; both Kurucz and Butler model atmospheres have been used. It turns out that there is one wavelength point (3830 Å in the Kurucz wavelength grid) in the Balmer region where the Butler model is severely off; as a test, fits with both the Kurucz and Butler spectra have been performed excluding this observed wavelength point (models 3 and 4), in order to better compare the 2 sets of theoretical spectra. Also in this case the Kurucz models provide the lower (reduced) χ^2, and therefore they will be adopted from now on as the standard theoretical spectra. Morever, the results for the fitted parameters obtained with the Kurucz spectra are completely insensitive to the inclusion or not of this wavelength point.

It is interesting to note that the [m/H] value found with Butler data is higher than with the Kurucz ones. This is related to the fact that the adopted solar Fe abundance adopted by Butler is lower (more in agreement with the currently accepted value, see previous discussion) than in the case of Kurucz ATLAS 9 models. The difference of 0.21 dex in the [m/H] value derived from the fitting is exactly the same as the difference in the adopted solar iron content between the two sets of model atmospheres. This is consistent with the claim by Fitzpatrick & Massa (1999) that the Fe abundance is the main parameter responsible for the UV spectral signature of the total metal content. In this respect it is also worth pointing out that in Table 2 we summarize the G98a and G98b results showing their derived [Fe/H] abundances. We believe that these [Fe/H] abundances are derived applying (as suggested by Fitzpatrick & Massa 1999) a correction to the derived [m/H] values taking into account the difference between the ATLAS 9 solar iron abundance and the Grevesse & Noels (1993) one; this should be taken into account when comparing results in Table 2 with the results listed in Table 3.

A remark must be also made regarding the high values of χ^2 obtained for models 1–4 which would indicate that they are not a good representation of the observations. G98a find a reduced χ^2 "close to one" also using Kurucz spectra. It seems likely that the difference is not due to the theoretical spectra, but rather to the assigned observational errors. In fact, the errors associated with the FOS spectrum are formal errors only, and do not include the error due to sky and background subtraction and flat field errors (see the FOS handbook). Furthermore, the FOS spectrum was binned. However, the wavelength points are not independent as each point was observed by several diodes in the FOS spectrograph. The errors in the FOS spectrum are therefore underestimates, but it is not simple to calculate the true error for each wavelength point. We therefore chose to scale all errors by a factor 1.5, to give a reduced χ^2 of approximately 1.0 for the standard model. This also allows a direct comparison of the derived errors with G98a.

5.2. Models 5–16

Model 5 represents the *reference model*, that is, the reference case with Kurucz spectra plus the scaling of the errors described above. The validity of scaling the errors is demonstrated by the fact that the values for the parameter are essentially unchanged (within 1σ) with respect to model 1. Only the errors on the derived quantities are increased; this probably makes these errors a conservative estimate of the real errors. Comparison of model 5 with the previous results in Table 2 shows that the results are in better agreement with G98b than with G98a. However, since in our case different constraints on the reddening law are used, and also the $(V-I)$ is added to the wavelength range to be fitted with theoretical spectra, it is difficult to compare the results directly. Such an attempt will be made with model 21.

In model 6 a fit is performed as for model 5 (but without the FOS spectrum point at 3830 Å) using the Butler model atmospheres. Significant differences are derived for some of the extinction parameters as well as for the distance (the scaling factor $\left(\frac{r_A}{d}\right)^2$) and the effective temperature of the primary component. The resulting χ^2 is however larger than when using ATLAS 9 spectra.

Models 7–16 show the influence of 9 sources of errors on the results of model 5. In models 7 and 8, c_1 and c_2 are increased by their respective 1σ uncertainty; models 9–12 investigate the uncertainty in the binary parameters, as derived from the radial velocity and lightcurve solution, while model 13 investigates the influence of the overall absolute photometric calibration on the distance. This calibration error nominally is 3% according to the FOS handbook, due to the uncertainties on the White Dwarf model–based reference flux system and several other instrumental and observational issues. For individual observations this error may be larger. Remarkably enough, the error on the derived parameters appears dominated by the fitting procedure and not by errors on the constraints. In model 14, the spectrum beyond 3240 Å is decreased by 1% to simulate possible offsets between the different parts of the FOS spectrum, while in models 15 and 16 the constraints on $(B-V)$ and $(V-I)$ are changed by 0.01 mag to simulate the absolute photometric error. The derived parameters are in agreement, within the respective error bars, with the results of model 5.

5.3. Models 17–22

In models 17–19, as a test, we consider the reference case plus rescaled errors, but excluding from the fit the observed $(V-I)$ value. We employed the three different sets of theoretical spectra described in Sect. 4.1 because in this case the Hubeny TLUSTY spectra cover all the relevant wavelength range. It is interesting to notice for model 17 that the exclusion of $(V-I)$ from the fit produces a difference at the level of 1.2σ for the derived values of $E(B-V)$, R and $\left(\frac{r_A}{d}\right)^2$. In the hypothesis that the ATLAS 9 models are a correct representation of the actual stellar spectra, at least for this kind of stars, this occurrence implies that there is information in the $(V-I)$ colour which must be taken into account when deriving the stellar properties. In this respect it is unfortunate that there are no data at longer wavelengths suited to be used in the fitting procedure.

The same fit with Butler spectra (model 19) provides a higher χ^2 with respect to Kurucz data. The derived distance is extremely short, significantly different from the reference model. The fit using TLUSTY spectra (model 18) provides an even higher χ^2. In particular, the fit in the 1450–1650 Å region is unsatisfactory. TLUSTY spectra provide by far the longest distance and lowest reddening, metallicity (especially considering the fact that the solar

Fe content in TLUSTY spectra is 0.17 dex lower than in the ATLAS 9 ones and 0.04 dex larger than for Butler models), effective temperature and R.

So far, the broad-band photometry of UPW98 was used because it included $(V-I)$. Model 5 fits well these constraints: $(B-V) = -0.135$ versus the observed value of -0.129 ± 0.015, and $(V-I) = -0.110$ versus the observed value of -0.125 ± 0.015, while $V = 14.187$ is predicted within 1.4σ of the observed value 14.16 ± 0.02. Model 20 is similar to model 17, with the only exception than in this case we used the observed $(B-V) = -0.172 \pm 0.013$ from Nelson et al. (2000) as constraint. This leads to a longer distance to the binary, the parameter $\left(\frac{r_A}{d}\right)^2$ being 1.4σ lower than in the case of model 5. The χ^2 is only slightly higher than in the case of model 17, but the observed V and $(B-V)$ values considered in this case are more poorly reproduced with respect to model 5 or model 17. In particular, the predicted $(B-V)$ value is about 2σ different from the observed one.

Model 21 is probably the closest to what is our understanding of what G98a did, that is, model 6 but fixing $R = 3.1$ and not using $(V-I)$ as constraint. However, reddening and distance differ significantly from those quoted in G98a. In particular, we get a longer distance and lower reddening; we were unable to trace the reasons for this difference. While the values of the derived parameters, with the exception of the metallicity, are consistent within 1σ with the results from the reference model, it is remarkable the difference with respect to the distance derived from model 17. The only constraint changed between these two cases is that in model 21 we kept R fixed at 3.1, while in model 17 R was a free parameter.

Model 22 is as model 21, with the inclusion of the observed $V = 14.16 \pm 0.02$ as additional constraint to the fit. The derived parameters are almost exactly the same in both models.

6. Discussion

We will now discuss the results obtained in the previous section, with particular emphasis on the consistency of the derived parameters for the reference model.

6.1. The distance to HV 2274

As previously explained, our reference model is model 5, which has the maximum wavelength coverage – from the UV to the near infrared – of the HV 2274 spectrum, and makes use of the set of theoretical spectra which provides the lower χ^2 value. In Figs. 1 and 2 we show, for model 5, the fit of the theoretical spectra to the FOS one, and the resulting UV and optical normalized extinction curve.

The final value for $\left(\frac{r_A}{d}\right)^2$ is that of model 5. The final error estimate comes from the formal error in the model 5 result, added in quadrature to the squared differences of the parameter values of model 5 with those of models 7–16, and the additional error due to the error in r_A. The result is $\left(\frac{r_A}{d}\right)^2 = (2.05 \pm 0.12)\ 10^{-23}$. This corresponds to a linear distance of 49.10 ± 1.44 kpc, or a true distance modulus of 18.46 ± 0.06.

6.2. The distance to the center of the LMC

To obtain the distance to the center of the LMC, the location of the binary with respect to the LMC center has to be taken into account. The geometry of the LMC can be described by an inclined disk, and one therefore has to consider the distance from the plane of that disk to the plane of the sky through the center of the LMC at the position of the binary, and the fact that the binary may be behind or in front of the plane of the disk. G98a assume that HV 2274 is 1.1 kpc behind the center of the LMC, based on the parameters of Schmidt-Kaler & Gochermann (1992).

Various authors have described the geometry of the LMC with a thin disk and derived the position angle (θ) of the line-of-nodes and inclination angle (i). The relevant coordinate transformation to go from observed right ascension and declination to a rectangular coordinate system in the plane of the sky, and to a similar one rotated by θ and i are given in Weinberg & Nikolaev (2000). Table 6 gives estimates of the distance of the LMC plane to the center of the LMC for various accurate estimates of θ and i, using the coordinate system by Weinberg & Nikolaev (2000). Because of the different orientations and definition of positive inclination the values in the table may differ by 90° with respect to the values quoted in the original reference.

The mean of these 5 determinations is 0.88 kpc; the average of the highest and lowest value is 0.89 kpc and the median is 0.82 kpc. The adopted difference in distance is 0.9 ± 0.3 kpc[2]. The error does not come from the internal errors of each of the determinations, but from the spread among the values itself, and the difference between the lowest and highest value has been assumed to correspond to 3σ.

It is unknown if HV 2274 is in front or behind the LMC plane. The vertical scale height of the LMC disk is small however, between 100 and 300 pc (see the discussion in Groenewegen 2000). The largest value is taken here, and added to the error mentioned above, to give the final result that HV 2274 is located 0.9 ± 0.5 kpc behind the LMC center. Considering a DM to HV 2274 of 18.46 ± 0.06, the DM to the LMC center 18.42 ± 0.07.

[2] As an aside we did the same for SN 1987A. The shortest distance (SN 1987A - LMC Center) is -0.64 kpc [for the parameters of Schmidt-Kaler & Gochermann 1992], and the largest is -0.15 kpc [for the parameters of Groenewegen 2000]. Based on all 5 determinations, the LMC plane at the location of SN1987A is 0.4 ± 0.2 kpc in front of the LMC center.

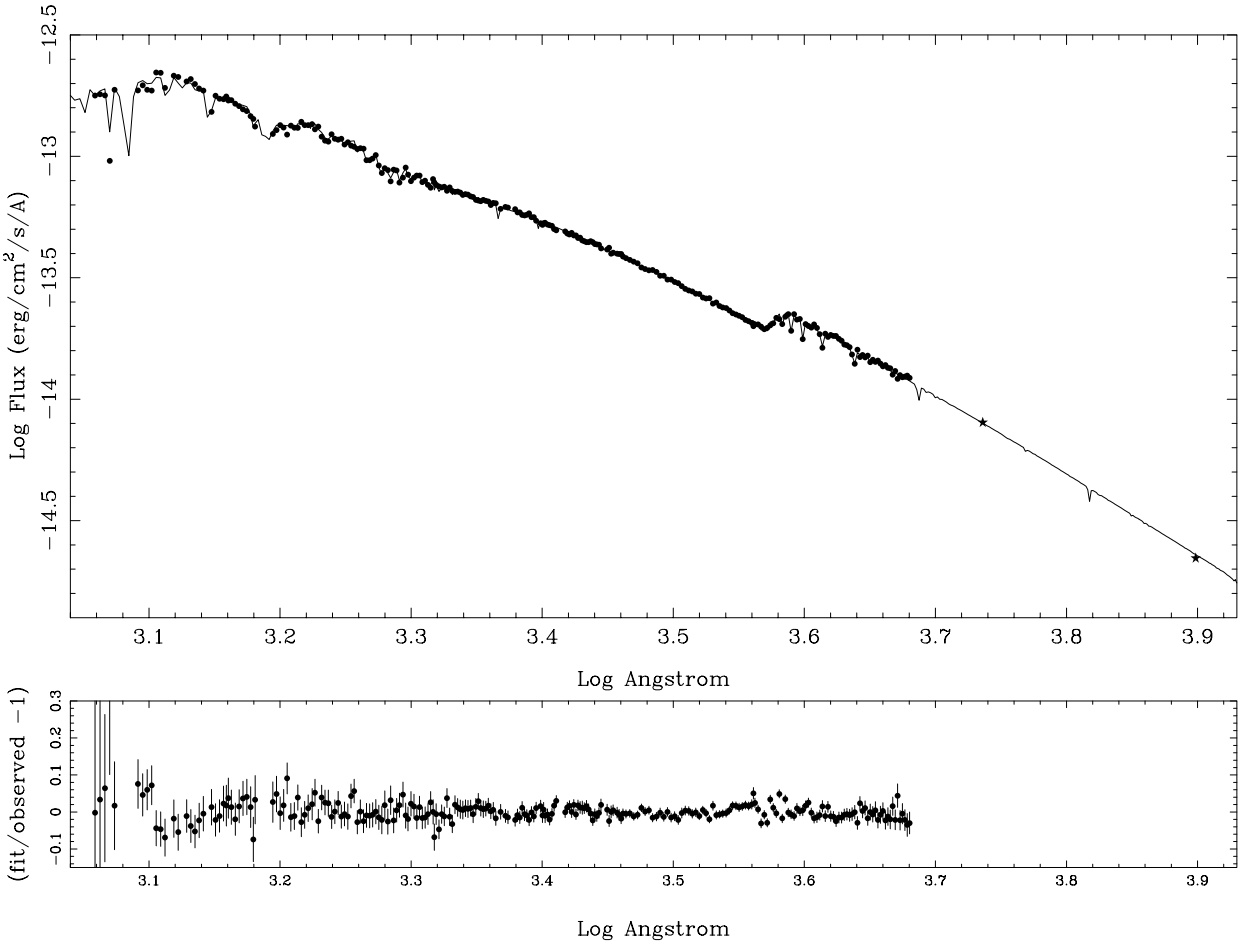

Fig. 1. Best fit to the observed data (model 5). In the lower panel the residuals are plotted, with the error in the individual observation. V and I are plotted at the effective wavelenghts calculated from folding the energy distribution with the filter response curves

Table 6. The distance (HV 2274 − LMC center)

θ (°)	i (°)	Reference	Δ (kpc)
258	38	Schmidt-Kaler & Gochermann (1992)	1.30
258	33	Feitzinger et al. (1977)	1.08
261	25	Weinberg & Nikolaev (2000)	0.82
296	18	Groenewegen (2000)	0.75
232	29	Martin et al. (1979)	0.47

6.3. The extinction curve towards HV 2274

From model 5 we get $x_0 = 4.67 \pm 0.04$, $\gamma = 1.27 \pm 016$, $c_3 = 2.03 \pm 0.58$, $c_4 = 0.66 \pm 0.10$ and $R = 3.06 \pm 0.14$ (where the errors are the internal errors due to the fitting procedure only); from Eqs. (6) and (7) one obtains $c_1 = -0.13 \pm 0.21$ and $c_2 = 0.72 \pm 0.07$. These values are consistent with the corresponding quantitites recently determined by Misselt et al. (1999) for their "LMC-Average Sample" of stars. Figure 2 shows the resulting normalised UV and optical extinction curve.

6.4. The reddening towards HV 2274

The value of $E(B-V)$ obtained from model 5 is $E(B-V) = 0.103 \pm 0.007$. It is important to notice that this value is different from the one derived by G98b ($E(B-V) = 0.120 \pm 0.009$) and from the determination by UPW98 ($E(B-V) = 0.149 \pm 0.015$) who used colour-colour $(U-B)-(B-V)$ relationships. Since we are using the $(B-V)$ (and $(V-I)$) photometric data by UPW98 as constraint for the spectrum fit we investigated the possibility that the reddening derived from the spectrum fit is inconsistent with HV2274 broad band photometry.

We followed the same procedure by UPW98 that is, to consider a local standard $(U-B)-(B-V)$ sequence of stars with the same spectral type as HV 2274, and derive the reddening from the displacement of the position of HV 2274 with respect to the standard sequence, for an assumed $E(U-B)/E(B-V)$ ratio. We used the same standard colour-colour sequence employed by UPW98 (for B-stars of luminosity class III), and a ratio $E(U-B)/E(B-V)$ derived from our adopted extinction law using the value of R derived from the fit (which is by the way very close to the standard value of 3.1).

By computing appropriate stellar models (using the same input physics and colour transformations as in Salaris & Weiss 1998 and a scaled-solar metal distribution) for solar metallicity and the metallicity derived from model 5, with masses around 12 $M_{\odot}$, we verified that the location of B stars on the $(U-B)-(B-V)$ plane does not vary in this metallicity range.

As for the $(B-V)$ colour of HV 2274 we used the value by UPW98, while for $(U-B)$ we derived the value from the FOS spectrum (see Sect. 4.2), since it covers the wavelength region spanned by this colour index. The $(U-B)$ colour derived from the spectrum is different from the value observed by UPW98. The FOS spectrum provides $(U-B) = -0.836 \pm 0.006$, while UPW98 measured $(U-B) = -0.905 \pm 0.04$. Nelson et al. (2000) measured $(U-B) = -0.793 \pm 0.031$ which is closer (but still inconsistent at the 1σ level) to the value derived from the FOS spectrum. From the colour-colour diagram we get $E(B-V) = 0.115 \pm 0.015$ which is consistent, within 1σ, with the value derived from model 5.

6.5. The metallicity of HV 2274

The value of [m/H] from the reference model, taking the formal error from the fit plus the external errors from models 7–16 is -0.38 ± 0.12. This is relative to the adopted iron abundance of 7.67 in the Kurucz models. This implies that the metallicity relative to the currently favoured solar iron abundance of 7.51 (Grevesse & Noels 1993) is [Fe/H] $= -0.22 \pm 0.12$. model 6 computed using Butler atmospheres has [m/H]$= -0.13$ relative to a solar abundance of 7.46, [Fe/H] $= -0.18$ relative to the solar abundance of Grevesse & Noels. These values are in good agreement with each other, but significantly more metal rich than the value of -0.42 ± 0.07 to -0.45 ± 0.06 found by G98a,b.

Observationally there are few direct iron abundance determinations for hot and young stars in the LMC. Haser et al. (1998) derived a metallicity of -0.3 and -0.1 dex for an O3III and O4I star in the LMC. Korn et al. (2000) determined the iron abundance in 5 non-supergiant B-stars, the average value being -0.42 ± 0.15. Both the values found by G98a,b and ours are consistent with these determinations.

6.6. The 2MASS data

As mentioned in Sect. 3 HV 2274 has been detected in the 2MASS $JHK_{\rm s}$ infrared survey. The observation date is $JD = 2451111.689$. From the ephemeris in Watson et al. (1992) a primary eclipse is predicted at $JD = 2451111.697 \pm 0.006$, taking into account the error in the time determination of the reference primary eclipse and the period. The shift of 0.008 ± 0.006 days, or 0.0014 in phase is negligible, also in light of the fact that phase shifts of up to 0.05 occur due to apsidal rotation (Watson et al. 1992).

In the optical the magnitude difference between out-of-eclipse and primary eclipse are 0.72, 0.71 and 0.70 mag in BVI, respectively (Watson et al. 1992). Naively, one might therefore expect a magnitude difference of about 0.69 in J. The difference between the observed 2MASS J and the model predictions is $(15.152 \pm 0.057) - (14.503 \pm 0.049) = 0.65 \pm 0.08$, where the error in the model comes from summing up all the error terms from models 6–17. This is in good agreement with the value extrapolated from the magnitude difference between out-of-eclipse and primary eclipse measured in the optical. However, as emphasised later, out-of-eclipse NIR photometry would be important in further constraining the parameters of the model.

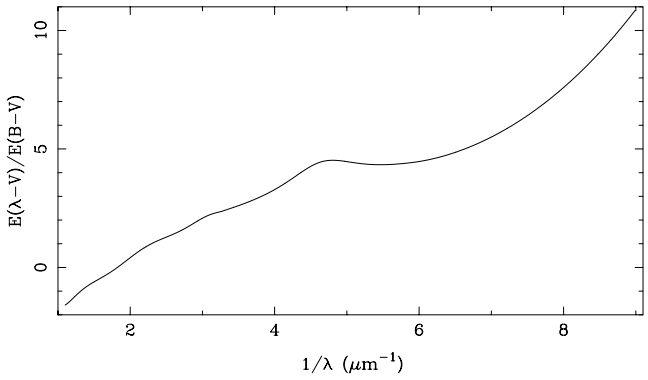

Fig. 2. UV and optical normalised extinction curve for the parameters of model 5

6.7. Final remarks

In this paper we have described and analyzed in detail the method used by G98a,b to derive the distance to the eclipsing binary HV 2274 in the LMC. We used various sets of theoretical spectra and broad band photometric data in the fitting procedure outlined in Sect. 4, and we found that Kurucz ATLAS 9 spectra best reproduce the observed spectrum of HV 2274. The selection of the wavelength range to be covered by the spectrum fit and the constraint on R play also a role in determining the outcome of the fitting procedure. We are now going to comment briefly about this point.

In the reference model we fitted HV 2274 FOS data plus $(B-V)$ and $(V-I)$ colours (from UPW98) using ATLAS 9 spectra, constraining the parameters c_1 and c_2 of the UV extinction law according to Eqs. (6) and (7) and keeping R as a free parameter. The use of $(V-I)$ is dictated by our desire to use all available information about the spectral energy distribution of HV 2274. The homogeneous $UBVI$ photometry by UPW98 makes it possible to cover all the spectral range from UV to near-infrared.

Neglecting $(V-I)$, that means, fitting a smaller wavelength range, induces a decrease by 0.10 mag in the distance modulus derived from the fitting procedure. If we consider the ATLAS 9 models as an accurate reproduction of the "real" spectra of B stars, this difference can be ascribed to the fact that there is information about the distance contained in the $(V-I)$ colour, and therefore

it must be included in the fitting procedure. Conversely, this result could also imply that ATLAS 9 spectra are inconsistent with observations at the longer wavelengths or that broad-band photometry and FOS spectrum are not homogeneously calibrated. In this respect, one should keep in mind that the $(U-B)$ value derived from the FOS spectrum is inconsistent with the $(U-B)$ determined by UPW98 and Nelson et al. (2000) and also that the $(U-B)$ values derived from the best-fit ATLAS 9 spectrum are systematically different by $\sim$0.03 mag with respect to the FOS colour (see Table 5).

In case of not considering $(V-I)$ for the spectrum fitting, keeping R fixed increases sensibly (0.09 mag) the derived distance modulus with respect to the case of having R determined by the fitting procedure, as shown by comparing the outcome of models 21 and 17. However, it is not clear why one should fix the value of R a priori, since it is known that it is subjected to variations within the LMC and within our galaxy. Finally, the use of the $(B-V)$ by Nelson et al. (2000) together with the FOS spectrum produces a distance modulus even larger (0.16 mag larger than the case of using UPW98 data). The quality of the fit is only marginally lower, and the reddening compares well with the value ($\sim$0.08) one would derive from the colour-colour diagram considering the Nelson et al. (2000) $(B-V)$ and the FOS $(U-B)$.

A last comment is that it is very unfortunate that the 2MASS infrared data happens to be taken during eclipse. The difference in predicted JHK between the different models is up to 0.15 mag (see Table 5). Therefore, accurate NIR photometry or even NIR spectroscopy at the 1% level is expected to give valuable additional constraints.

The conclusion is that the use of eclipsing binaries as distance indicators is powerful, but that a photometrically well calibrated data set covering a large wavelength region is essential. Furthermore, the discrepancies among the different theoretical model atmospheres is worrying and need further investigation.

Acknowledgements. It is a pleasure to thank Keith Butler (Munich Observatory) and Ivan Hubeny (Goddard Space Flight Center) for providing us with model atmospheres tailored to our specific needs, Ignasi Ribas for many helpful remarks, and Phil James for a preliminary reading of the manuscript.

This work is based on observations made with the NASA/ESA Hubble Space Telescope, obtained from the data archive at the Space Telescope Science Institute. STScI is operated by the Association of Universities for Research in Astronomy, Inc. under NASA contract NAS 5-26555.

This publication makes also use of data products from the Two Micron All Sky Survey, which is a joint project of the University of Massachusetts and the Infrared Processing and Analysis Center/California Institute of Technology, funded by the National Aeronautics and Space Administration and the National Science Foundation.

References

Beichman, C. A., Chester, T. J., Cutri, R., et al. 1998, PASP, 110, 367
Bessell, M. S. 1990, PASP, 102, 1181
Bessell, M. S., Castelli, F., & Plez, B. 1998, A&A, 333, 231
Carbon, D. F., & Gingerich, O. J. 1969, in Theory and Observations of Normal Stellar Atmospheres, ed. O. J. Gingerich (Cambridge, MA: MIT Press), 377
Cardelli, J. A., Clayton, G. C., & Mathis, J. S. 1989, ApJ, 345, 245
Cioni, M.-R., Loup, C., Habing, H. J., et al. 2000, A&AS, 144, 235
Cutri, R. M., Skrutskie, M. F., Van Dyk, S., et al. 2000, Explanatory Supplement to the 2MASS Second Incremental Data Release
Epchtein, N., Deul, E., Derriere, S., et al. 1999, A&A, 349, 236
Feast, M. W., 2001, in IAU Symposium 201, New cosmological data and the values of the fundamental parameters, ed. A. Lasenby, A. Wilkinson, in press [astro-ph/0010590]
Feast, M. W., & Catchpole, R. M. 1997, MNRAS, 286, L1
Feitzinger, J. V., Isserstedt, J., & Schmidt-Kaler, Th. 1977, A&A, 57, 265
Fitzpatrick, E. L. 1999, PASP, 111, 63
Fitzpatrick, E. L., & Massa, D. 1990, ApJS, 72, 163
Fitzpatrick, E. L., & Massa, D. 1999, ApJ, 525, 1011
Freedman, W. L., Madore, B. F., Mould, J. R., & Kennicutt, R. C. 1999, in Cosmological Parameters and the Evolution of the Universe, ed. K. Sato (Dordrecht), 17
Gibson, B. K. 1999, Mem. Soc. Astron. Italiana, in press [astro-ph/9910574v2]
Gray, D. F. 1992, The observations and analysis of stellar photospheres (Cambridge UP), 184
Grevesse, N., & Noels, A. 1993, in Origin and evolution of the elements, ed. N. Prantzos, E. Vangioni-Flam, M. Cassé, CUP, 14
Groenewegen, M. A. T. 2000, A&A, in press [astro-ph/0010298]
Guinan, E. F., Fitzpatrick, E. L., DeWarf, L. E., et al. 1998a, ApJ, 509, L21 (G98a)
Guinan, E. F., Ribas, I., Fitzpatrick, E. L., & Pritchard, J. D. 1998b, in Ultraviolet Astrophysics, beyond the IUE final archive, ed. W. Wamsteker, R. González Riestra, B. Harris, ESA SP-413, 315 (G98b)
Haser, S. M., Pauldrach, A. W. A., Lennon, D. J., et al. 1998, A&A, 330, 285
Hubeny, I. 1988, Computer Physics Comm., 52, 103
Hubeny, I., & Lanz, T. 1992, A&A, 262, 501
Hubeny, I., Hummer, D. G., & Lanz, T. 1994, A&A, 282, 151
Hubeny, I., & Lanz, T. 1995, ApJ, 439, 875
Kennicutt, R. C., Freedman, W. L., & Mould, J. R. 1995, AJ, 110, 1476
Koen, C., & Laney, D. 1998, MNRAS, 301, 582
Korn, A. J., Becker, S. R., Gummersbach, C. A., & Wolf, B. 2000, A&A, 353, 655
Kurucz, R. L. 1979, ApJS, 40, 1
Kurucz, R. L. 2000, http://cfaku5.harvard.edu/
Martin, W. L., Warren, P. R., & Feast, M. W. 1979, MNRAS, 188, 139
Milone, E. F., Stagg, C. R., & Kurucz, R. L. 1992, ApJS, 79, 123
Milone, E. F., Stagg, C. R., Kallrath, J., & Kurucz, R. L. 1994, BAAS, 184.0605

Misselt, K. A., Clayton, G. C., & Gordon, K. D. 1999, ApJ, 515, 128
Nelson, C. A., Cook, K. H., Popowski, P., & Alves, D. R. 2000, AJ, 119, 1205
O'Donnell, J. E. 1994, ApJ, 422, 158
Press, W. H., Flannery, B. P., Teukolsky, S. A., & Vetterling, W. T. 1992, Numerical Recipes (Cambridge UP)
Ribas, I., Guinan, E. F., Fitzpatrick, E. L., et al. 2000, ApJ, 528, 692
Saha, A., Sandage, A., Tammann, G. A., et al. 1999, ApJ, 522, 802
Salaris, M., & Weiss, A. 1998, A&A, 335, 943
Schmidt-Kaler, Th., & Gochermann, J. 1992, in Variable stars and galaxies, ed. B. Warner, ASP Conf. Ser. 30, ASP San Francisco, 203
Udalski, A., Szymański, M., Kubiak, M., et al. 1998a, AcA, 48, 1
Udalski, A., Pietrzyński, G., Woźniak, P., et al. 1998b, ApJ, 509, L25 (UPW98)
Watson, R. D., West, S. R. D., Tobin, W., & Gilmore, A. C. 1992, MNRAS, 258, 527
Weinberg, M. D., & Nikolaev, S. 2000, [astro-ph/0003204]
Wilson, R. E., & Devinney, E. J. 1971, ApJ, 166, 605